Journal of Nuclear Medicine, published on March 20, 2020 as doi:10.2967/jnumed.119.238790

The optimal imaging window for dysplastic colorectal polyp detection using c-Met targeted fluorescence molecular endoscopy

Authors and affiliations

Steven J. de Jongh[1]*, Josephina P.M. Vrouwe[2]*, Floris J. Voskuil[3], Iris Schmidt[1], Jessie Westerhof[1], Jan J. Koornstra[1], Marieke L. de Kam[2], Arend Karrenbeld[4], James C.H. Hardwick[5], Dominic J. Robinson[6], Jacobus Burggraaf[2], Ingrid M.C. Kamerling[2#], Wouter B. Nagengast[1#]

* *Both authors share first authorship*

Both authors share senior authorship

1. Department of Gastroenterology and Hepatology, University Medical Center Groningen, Groningen, The Netherlands;
2. Centre for Human Drug Research, Leiden, the Netherlands;
3. Department of Oral and Maxillofacial Surgery, University Medical Center Groningen, Groningen, The Netherlands;
4. Department of Pathology, University Medical Center Groningen, Groningen, The Netherlands;
5. Department of Gastroenterology and Hepatology, Leiden University Medical Center, Leiden, The Netherlands.
6. Center for Optical Diagnostics and Therapy, Department of Otorhinolaryngology and Head and Neck Surgery, Erasmus MC Cancer Institute, Rotterdam, the Netherlands;

Running title: c-Met fluorescence molecular endoscopy

Corresponding author. Wouter B. Nagengast, MD/PhD/PharmD. Department of Gastroenterology and Hepatology, University Medical Center Groningen, Hanzeplein 1, 9713GZ, Groningen, the Netherlands. Phone: +31(0)50-3612620; Fax: +31(0)50-3619306; w.b.nagengast@umcg.nl.

First authors. Steven J. de Jongh, MD. Hanzeplein 1, 9713 GZ, Department of Gastroenterology and Hepatology, University Medical Center Groningen, Groningen, the Netherlands. Phone: +31(0)50-3612620; Fax: +31(0)50-3619306; s.j.de.jongh@umcg.nl.

Josephina P.M. Vrouwe, MD. Centre for Human Drug Research, Zernikedreef 8, 2333 CL, Leiden, the Netherlands. Phone: +31(71)-5246400; Fax: +31(71)-5246499; jvrouwe@chdr.nl.

Author Contributions. SJdJ and JPMV designed the study, performed data acquisition, analyzed and interpreted data and drafted the manuscript. FJV and IS performed data acquisition, interpreted data and critically revised the manuscript. JJK and JW performed fluorescence molecular endoscopy procedures and critically revised the manuscript. AK performed and supervised the histopathological and immunohistochemistry analyses and critically revised the manuscript. MLdK contributed to the design of the study, analyzed data, and critically revised the manuscript. DJR analyzed and interpreted data and critically revised the manuscript. JCHH, JB and IMCK designed and supervised the study, interpreted data and critically revised the manuscript. WBN designed the study, performed fluorescence molecular endoscopy procedures, interpreted data and critically revised the manuscript. All authors have revised and approved the final manuscript.

ABSTRACT

Rationale: Fluorescence molecular endoscopy (FME) is an emerging technique that has the potential to improve the 22% colorectal polyp detection miss-rate. We determined the optimal dose-to-imaging interval and safety of FME using EMI-137, a c-Met targeted fluorescent peptide, in a population at high-risk for colorectal cancer.

Methods: We performed *in vivo* FME and quantification of fluorescence by multi-diameter single-fiber reflectance, single-fiber fluorescence spectroscopy in 15 patients with a dysplastic colorectal adenoma. EMI-137 was intravenously administered (0.13mg/kg) at a one-, two- or three-hour dose-to-imaging interval (N=3 patients per cohort). Two cohorts were expanded to six patients based on target-to-background ratios (TBR). Fluorescence was correlated to histopathology and c-Met expression. EMI-137 binding specificity was assessed by fluorescence microscopy and *in vitro* experiments.

Results: FME using EMI-137 appeared to be safe and well tolerated. All dose-to-imaging intervals showed significantly increased fluorescence in the colorectal lesions compared to surrounding tissue, with a TBR of 1.53, 1.66 and 1.74 respectively (mean intrinsic fluorescence ($Q \cdot \mu^f_{a,x}$) = 0.035 vs. 0.023mm^{-1}, P<0.0003; 0.034 vs. 0.021mm^{-1}, P<0.0001; 0.033 vs. 0.019mm^{-1}, P<0.0001). Fluorescence correlated to histopathology on a macroscopic and microscopic level, with significant c-Met overexpression in dysplastic mucosa. *In vitro,* a dose-dependent specific binding was confirmed.

Conclusion: FME using EMI-137 appeared to be safe and feasible within a one-to-three hour dose-to-imaging interval. No clinically significant differences were observed between the cohorts, although a one-hour dose-to-imaging interval was preferred from a clinical perspective. Future studies will investigate EMI-137 for improved colorectal polyp detection during screening colonoscopies.

Keywords. Optimal imaging window; fluorescence molecular endoscopy; colorectal polyp detection; colorectal cancer; EMI-137 targeting c-Met.

INTRODUCTION

The majority of colorectal cancers (CRC) develop through the adenoma-to-carcinoma sequence. (*1*) Therefore, early detection of premalignant polyps such as adenomas and sessile serrated polyps could improve patient outcome. (*2*) To date, the gold standard for premalignant lesion detection is high definition white-light endoscopy (HD-WLE). Although HD-WLE has significantly contributed to the success of screening for and prevention of CRC, it also has limitations. (*3*,*4*) Factors such as inadequate bowel preparation and skill and expertise of the endoscopist may cause reduced sensitivity, leading to an adenoma detection miss-rate of up to 22% in the general population and 55% in patients with Lynch syndrome. (*5*,*6*) Location (i.e. ascending colon) and morphological characteristics of the adenoma such as small size (i.e. less than 10mm) or flat shape are notorious for higher miss-rates. (*7*)

This emphasizes the need for a novel imaging technology to reduce the high detection miss rates. Fluorescence molecular endoscopy (FME) makes use of administration of targeted fluorescent tracers that enable the visualization of specific markers that are overexpressed on the target of interest. Combining HD-WLE technique to visualize morphological mucosal abnormalities with FME to visualize real-time biological characteristics of cells has the potential to improve polyp detection rates. (*8*–*10*)

One of the markers that becomes significantly overexpressed as the degree of dysplasia progresses in the colorectal adenoma-to-carcinoma sequence, is c-Met. (*11*) c-Met is a receptor tyrosine kinase that binds to its ligand hepatocyte growth factor and activates several downstream signaling pathways involved in proliferation, motility, migration and invasion. (*11*,*12*) The fluorescently labelled peptide EMI-137 (previously: GE-137), is a water-soluble 26-amino acid cyclic peptide that specifically binds to human c-Met with high affinity. (*8*) It has a peak excitation and emission wavelength of 653 and 675nm respectively and favorable pharmacokinetic properties that enable rapid tissue biodistribution, with a background clearance half-life of approximately 2 hours and 30 minutes.

Previously, intravenous (i.v.) administration of EMI-137 three hours prior to colonoscopy showed the potential to detect additional polyps that were initially missed by conventional fiber-based WL colonoscopy. (*8*) To expand the clinical applicability of EMI-137 for future phase II/III trials, we determined its optimal dose-to-imaging interval for colorectal polyp detection using FME in parallel to HD-WLE, with quantification of fluorescence using multi-diameter single-fiber reflectance, single-fiber fluorescence (MDSFR/SFF) spectroscopy. In addition, the safety and tolerability of EMI-137 were investigated in a group of patients at high suspicion of CRC.

MATERIALS AND METHODS

Study Design

This study was approved by the Ethics Committee 'Foundation Beoordeling Ethiek Biomedisch Onderzoek', The Netherlands. All patients signed written informed consent. Patients were found eligible for study participation if they were 18 years of age or older and scheduled to undergo a diagnostic or therapeutic endoscopy for a colorectal adenoma containing at least low-grade dysplasia (LGD). Female patients had to be either surgically sterile, post-menopausal or pre-menopausal with a negative urine pregnancy test. The study was registered in the European Clinical Trials Register (2016-002827-27) and conducted according to the Declaration of Helsinki at the University Medical Center Groningen, Groningen, The Netherlands, between October 2017 and September 2018.

In Vivo Endoscopy Procedures

EMI-137 was administered as a single i.v. bolus injection of 0.13mg/kg in a solution of 4.8mg/ml at either one-, two- or three-hours prior to endoscopy, initially with three patients per cohort (Fig. 1). All endoscopic procedures were performed by a board-certified gastroenterologist using a clinical HD video-endoscope (CF-HQ190L/I, EVIS EXERA III, Olympus Corporation, Tokyo, Japan) after standard bowel preparation. Therapy consisted of a piecemeal polypectomy,

endoscopic mucosal resection (EMR), endoscopic submucosal dissection (ESD) or endoscopic full-thickness resection (eFTR), depending on lesion location, size and characteristics. A 650nm short-pass filter (Chroma Technology Corp., Bellows Falls, VT, USA) was installed in the Olympus xenon light-source (CLV-190, EVIS EXERA III, Olympus Corporation, Tokyo, Japan) to prevent unintended excitation of EMI-137.

Fluorescence was visualized *in vivo* using the SurgVision Explorer Endoscope (SVEE, SurgVision B.V., Groningen, The Netherlands), a real-time fluorescence imaging system connected to a flexible fiberscope that can be inserted through the clinical HD video-endoscope. The SVEE consists of a white-light emitting diode and two class III-b lasers optimized for EMI-137 visualization (excitation wavelength: 653nm), which simultaneously produces a white-light, fluorescence and overlay image.

During FME, adenoma visibility was qualitatively described as ‘clearly increased’, ‘mildly increased’ or ‘same as background’ compared to the surrounding normal tissue, by consensus between the gastroenterologist and the investigator. To confirm *in vivo* visualized fluorescence imaging results, fluorescence intensities were subsequently quantified *in vivo* using MDSFR/SFF spectroscopy, an optical technique that corrects for the influence of tissue optical properties and therefore enables determination of the EMI-137 intrinsic fluorescence values (Fig. 2A). Briefly, another fiber-bundle was inserted to determine the tissue absorption coefficient and reduced scattering coefficient at the excitation wavelength (650nm) and the emission band of the fluorophore, Cy5** (600–800nm) through direct-contact MDSFR measurements. Subsequently, a SFF spectrum was acquired. After the clinical procedure, the intrinsic fluorescence values ($Q \cdot \mu^{f}_{a,x}$) of Cy5** in EMI-137 were calculated. (*10*,*13*–*15*)

Depending on the endoscopy procedure length, multiple FME and MDSFR/SFF spectroscopy measurements were acquired of each lesion and the surrounding normal tissue every 30 minute. In case *in vivo* MDSFR/SFF measurements could not be acquired due to the

lesion location (this fiber-bundle cannot be inverted), measurements were obtained *ex vivo* directly after resection.

Outcome Parameters

Safety and tolerability. Vital signs, the injection site and the occurrence of (serious) adverse events based on the commmon toxicity criteria for adverse events were monitored at regular time-points. Follow-up took place up to 24 to 48 hours after EMI-137 administration.

In vivo target-to-background ratio (TBR) analysis. Regions-of-interest (ROI) of the lesion and surrounding normal colorectal tissue were delineated on one-to-four representative white-light images per patient at approximately the same distance from the fiber, depending on image availability and quality. Subsequently, mean fluorescent intensities (MFI) were calculated as total counts per ROI pixel area using Fiji/ImageJ software (version 2.0.0-rc-68/1.52h). The lesion MFI was divided by the surrounding normal tissue MFI to determine target-to-background ratios (TBR). In addition FME image analysis, quantified intrinsic fluorescence values from the *in vivo* MDSFR/SFF spectroscopy measurements were analyzed, correlated to histopathology and similarly a TBR was calculated for each time-point per patient.

Interim analysis. An interim analysis was performed after the first nine patients to evaluate EMI-137 safety data and to determine the TBR using FME and MDSFR/SFF spectroscopy for each cohort. The two cohorts with the optimal TBR were expanded to six patients per cohort. In case of comparable TBRs for all three cohorts, the one- and two-hour cohort were to be expanded to six patients per cohort, as this was preferred from a clinical perspective.

Ex Vivo Validation

After resection, histopathological processing and examination was performed according to standard clinical protocol of the UMCG by a board-certified gastrointestinal pathologist, blinded for fluorescence imaging results.

Correlation of Fluorescence and Histopathology. A maximum of four 4μm tissue sections per patient were selected for further analyses, based on section quality and the simultaneous presence of dysplasia and surrounding normal crypts. After xylene deparaffinization, tissue sections were air dried and scanned using the Odyssey CLx fluorescence scanner (LI-COR Biosciences Inc, Lincoln, NE, USA), directly followed by hematoxylin/eosin (H/E) staining, to allow a precise correlation of fluorescence with histology. MFIs were measured as total counts per ROI pixel area for dysplastic mucosa and surrounding normal mucosa based on histological delineation by the pathologist.

Immunohistochemistry. A SP44 rabbit monoclonal primary antibody directed against the membranous and cytoplasmic c-Met epitope was used to perform c-Met immunohistochemistry using the BenchMark ULTRA system (Ventana Medical Systems, Oro valley, Arizona, USA) according to standard clinical protocol of the UMCG. Membrane-localized staining intensities were semi-quantitatively scored as negative (0), weak (1+), moderate (2+) or strong (3+) in dysplastic and surrounding normal colorectal mucosa by the pathologist. A 2+/3+ score was considered positive for c-Met overexpression.

Fluorescence Microscopy. Fluorescence microscopy was performed on one representative 4μm tissue section per patient, to evaluate the accumulation of EMI-137 on a microscopic level, as described previously. (*15*,*16*) A DM6000 fluorescence microscope coupled to a DFC360FX camera (Leica Biosystems GmbH, Wetzlar, Germany) was applied using the same settings per magnification on the A (FITC, autofluorescence), I (DAPI, nuclei) and Y5 (Cy5, i.e. EMI-137) filter cube.

Validation side study. Several *in vitro* experiments were performed on a high c-Met overexpressing (HT-29) and a negative c-Met expressing (SW-480) cell line to confirm EMI-137 binding specificity (described in Supplemental Material). (*17*)

Statistical Analyses

Descriptive statistics were applied to the patient demographics. For normally distributed data, mean values with standard deviation were used and a Student T test (paired data) was used to test for significance. Not normally distributed data is presented as median values with interquartile range (IQR) and a Wilcoxon (paired data) or Mann-Whitney U (independent data) test was used to test for significance. P-values <0.05 were considered statistically significant. Statistical analyses and graph design were performed using GraphPad Prism (version 8.0, GraphPad Software Inc, San Diego, California, USA).

RESULTS

Study Population

A total of 19 patients signed informed consent and were screened for study participation, 16 were found eligible for inclusion. The mean age was 62 years (range 59-73, (Table 1)). All 16 patients received an i.v. bolus injection of 0.13mg/kg EMI-137. Fourteen patients underwent an intended therapeutic procedure (three piecemeal polypectomies, four EMRs, six ESDs and one eFTR), one patient a diagnostic procedure, and in one patient the colonoscopy was prematurely aborted due to the patient's discomfort. Histological assessment of the resected lesions showed that all lesions were tubular adenomas that contained at least LGD. High grade dysplasia (HGD) was present in five tubular adenomas (31.2%) and adenocarcinoma in another three lesions (18.8%; (Table 1)).

Safety and Tolerability

No clinically significant changes in vital signs nor any skin abnormalities at the injection site were observed after administration of EMI-137 in any of the patients. One possibly related grade-1 adverse event (hypotension after anesthesia) and one possibly related grade-2 adverse event (mild allergic reaction, multiple hours after EMI-137 administration) were observed. Two serious adverse events occurred, both were iatrogenic perforations of the large intestine, which were

considered not related to EMI-137 or any study-related procedures, but to the therapeutic endoscopy procedure (sigmoid perforation during eFTR and rectum perforation during re-ESD in previously performed EMR area).

In Vivo Endoscopy Procedures

FME was performed in 15/16 patients. In one patient the endoscopy procedure was prematurely aborted, as the cecum polyp could not be reached due to the patient's discomfort. This patient received a polypectomy under propofol sedation at a later stage and was replaced in the study. The planned interim analysis after enrolment of the first nine patients showed comparable TBRs for all three time intervals regarding FME images and MDSFR/SFF spectroscopy measurements (data not shown). The one- and two-hour time interval cohorts were expanded to six patients each, because of clinical preference.

The dose-to-imaging time intervals of each cohort ranged from 0:54-1:28 hours (one-hour cohort), 1:50-2:33 hours (two-hour cohort) and 2:41-3:20 hours (three-hour cohort). During endoscopy, a total of 16 lesions were detected in 15 patients. The median adenoma size estimated during colonoscopy was 3.0 cm (range 1.5-5.5cm). Fluorescence was qualitatively assessed *in vivo* as clearly increased in 5/16 adenomas (31%), mildly increased in 8/16 adenomas (50%) and the same as the background in 3/16 adenomas (19%) based on FME images. The three lesions that were assessed to have the same fluorescence as the background could be identified using fluorescence due to their morphological characteristics. Representative FME images are shown (Fig. 3).

A total of 74 representative FME images acquired at different time-points from the 16 lesions, were analyzed to determine the TBR at each time interval. All lesions showed increased fluorescence compared to surrounding normal colorectal tissue, with a median TBR of 2.18 (IQR 0.87), 1.62 (IQR 0.51) and 1.43 (IQR 0.75) for the one-, two- and three-hour dose-to-imaging intervals respectively (Fig. 4).

In addition to the FME TBRs, *in vivo* direct contact MDSFR/SFF spectroscopy measurements were analyzed using a post processing algorithm to quantify the intrinsic fluorescence values by correcting for the optical properties in 14/16 lesions. MDSFR/SFF spectroscopy measurements of the remaining two lesions were performed *ex vivo* directly after adenoma resection, since *in vivo* measurements were not feasible for technical reasons. Quantified intrinsic fluorescence ($Q \cdot \mu^f_{a,x}$) was significantly higher in the adenomas compared to surrounding normal tissue for the one-hour cohort (0.035±0.0023 vs. 0.023±0.0024mm^{-1}, P<0.0003), two-hour cohort (0.034±0.0020 vs. 0.021±0.0014mm^{-1}, P<0.0001) and three-hour cohort (0.033±0.0023 vs. 0.019±0.0023mm^{-1}, P<0.0001; Fig. 2B). Quantified fluorescence values in the adenomas remained consistent from one- to at least three-hours. In contrast, a slight decreasing trend was observed for the quantified fluorescence values in normal colorectal tissue (Fig. 2B). As a result, the spectroscopy TBRs slightly increased over time, with a mean TBR of 1.53±0.21, 1.66±0.07 and 1.74±0.16 for the one-, two- and three-hour cohort respectively (Fig. 2B, right axis).

When comparing FME TBRs with MDSFR/SFF spectroscopy TBRs, no statistically significant differences were observed, except for the one-hour cohort, in which the FME TBRs were higher than the MDSFR/SFF spectroscopy TBRs (2.18 versus 1.54, P=0.038; Fig. 4). The MDSFR/SFF spectroscopy values that were corrected for the tissue scattering and absorption coefficients showed less variation compared to the values of the FME images.

Ex Vivo Validation

The correlation between fluorescence intensities, histology and c-Met expression was further evaluated *ex vivo*. In accordance with the *in vivo* results, dysplastic or cancerous mucosa showed significantly increased fluorescence compared to the surrounding normal mucosa on 4μm tissue sections for each cohort, with a median TBR of 1.69 (IQR 0.49; P=0.0398), 1.43 (IQR 0.37;

P=0.0020) and 1.46 (IQR 0.16; P=0.0156) for the one-, two- and three-hour cohort respectively (Fig. 5A).

c-Met immunohistochemical analysis demonstrated a moderate (2+, 72.2%) to strong (3+, 27.8%) membrane overexpression in dysplastic mucosa, whereas normal colorectal mucosa showed a negative (0+, 53.8%) to weak (1+, 46.2%) physiological membrane staining (Fig. 5B).

Finally, fluorescence microscopy showed increased fluorescence intensities in the dysplastic or cancerous colorectal crypts compared to surrounding normal colorectal crypts (Fig. 5C). The fluorescence signal clearly accumulated in the proximity of the cell membranes of the dysplastic cells. Surrounding normal tissue showed significantly lower fluorescence intensities, with a more stromal localization.

To further investigate EMI-137 binding specificity, *in vitro* experiments were performed. Immunohistochemistry and Western Blotting confirmed c-Met expression in HT-29 cells and minimal c-Met expression in SW-480 cells. Fluorescence microscopy revealed EMI-137 derived fluorescence on the surface of the HT-29 cells, whereas SW-480 cells showed negligible levels of fluorescence (Supplemental Figs. 1A and 1B). Flowcytometry analysis confirmed a dose-dependent membrane binding of EMI-137 in HT-29 cells, in contrast to SW-480 cells This was supported by a c-Met receptor saturation experiment using EMI-137 and the non-fluorescent unlabeled peptide (AH111972), showing blocking of the c-Met receptors and consequently, significantly lower MFIs only in the HT-29 cells (Supplemental Fig. 1C).

DISCUSSION

In this study, we demonstrate that FME using 0.13mg/kg EMI-137 administered one-, two- or three-hours prior to colonoscopy appears to be safe and feasible for the detection of colorectal polyps. *In vivo* FME results were confirmed by quantification of intrinsic fluorescence using MDSFR/SFF spectroscopy, showing significantly higher fluorescence in all lesions compared to surrounding normal colorectal tissue at each time interval. No clinically significant differences were

observed between the investigated time-cohorts based on extensive *in* and *ex vivo* analyses. Therefore, we conclude that FME using EMI-137 can be performed within a one- to three-hour timeframe, which expands the clinical applicability of EMI-137.

The use of FME to improve polyp detection by serving as a '*red-flag*' endoscopic imaging technique has been previously investigated using different fluorescent tracers, though several factors have hampered further clinical translation. (*9*,*10*) Firstly, the near-infrared fluorescent (NIRF) tracer bevacizumab-800CW targeting vascular endothelial growth factor-A (peak emission 792nm) has unfavorable pharmacokinetics that require a dose-to-imaging interval of 2-3 days, which limits application in a CRC screening population. (*10*) Secondly, the fluorescent peptide KCC*-FITC (peak emission 519nm), which binds to sessile serrated adenomas with a V600E point-mutation in BRAF, was evaluated using post-processing software. However, this limits *real-time* lesion identification in parallel to HD-WLE. (*9*) In addition, KCC*-FITC has a peak emission in the visible light spectrum, which reduces specificity due to higher autofluorescence levels compared to NIRF imaging. Besides i.v. administration, topical tracer administration has been evaluated as well during colonoscopy, although this rarely achieves complete mucosal coverage and tracer binding is affected by bowel preparation adequacy. (*18*) To overcome these limitations, we used a NIRF peptide with a relatively low molecular-weight and therefore favorable pharmacokinetic properties that allows adenoma identification within a timeframe of one- to at least three-hours after i.v. administration.

To identify the most optimal dose-to-imaging interval, quantification of fluorescence is important in early phase clinical FME trials, since fluorescence intensities observed by FME alone are affected by tissue optical properties and technical factors like camera sensitivity, imaging distance and illumination heterogeneity. (*19*) The addition of MDSFR/SFF spectroscopy as a confirmatory technique provides objective and consistent intrinsic fluorescence values through direct contact measurements that are corrected for the scattering and absorption coefficients of the tissue. (*10*,*13*–*15*) The significance of this was emphasized in the three adenomas that were

qualitatively assessed to have the same fluorescence as the background during FME, while MDSFR/SFF spectroscopy measurements showed a significant difference in intrinsic fluorescence values. Although MDSFR/SFF spectroscopy measurements are currently calculated using a post-processing algorithm, the results of this study further support its development as a complementary technique to FME.

In line with literature, our immunohistochemical analysis confirmed that c-Met is indeed a suitable marker for colorectal adenoma detection, as we observed a clear c-Met membrane overexpression in dysplastic and cancerous mucosa. (*11*,*12*) Although there is heterogeneity in the c-Met overexpression in the adenomas, this did not influence macroscopic fluorescence imaging results (Fig. 5). *In vivo* visualized and quantified fluorescence intensities remained consistent over time, indicating specific binding of EMI-137. In addition, the quantified intrinsic fluorescence values did not seem to further increase after one hour (Fig. 2B), suggesting that the current dose of 0.13mg/kg already saturates the available c-Met receptors one hour after administration. Interestingly, the background fluorescence levels slightly decreased over time, which was presumably caused by clearance of unbound EMI-137 (clearance half-life: ~2h30m). (*8*) A lower tracer dose might further decrease background fluorescence, while still saturating the available c-Met receptors, thereby potentially enhancing TBRs and improving sensitivity.

To date, integrated video-endoscopes that enable highly-sensitive near-infrared fluorescence imaging in parallel to HD-WLE have not been developed. We applied a NIRF endoscopy system that has the potential to be used clinically, since the use of the fiber-based SVEE enabled simultaneous HD-WLE and FME. This required installation of a short-pass filter in the standard Olympus white-light source, which prevents excitation of EMI-137 by the Olympys white-light source due to an overlap with the excitation spectrum of EMI-137. The SVEE fiber-probe consists of 10.000 fibers, allowing sufficient resolution for co-localizing fluorescence intensities to HD-WLE images for the current study design. However, increasing the number of fibers to 30.000 would improve white-light image quality and facilitate further clinical translation of

EMI-137 during screening colonoscopies. (*10*,*15*,*16*) In addition, the red laser-light was visible on the HD-WLE images from the clinical video-endoscope, influencing HD-WLE image quality. This is a phenomenon that has not been described previously when using bevacizumab-800CW, a fluorescent tracer that emits fluorescence further in the near-infrared light spectrum. (*10*,*15*,*16*) Alternatively, installation of a short-pass filter in the tip of the endoscope or pulsed acquisition could also prevent this.

In this study, FME was used to visualize fluorescence during endoscopy, while MDSFR/SFF spectroscopy was used to quantify intrinsic fluorescence values by correcting for tissue optical properties. Ultimately, clinicians need a technique that provides *real-time* objective information, preferably by combining these methods *in vivo*, to reliably guide the endoscopist during screening colonoscopies.

As the aim of this study was to determine the optimal dose-to-imaging interval for EMI-137, only patients with an advanced adenoma detected during a previous colonoscopy were included. As a result, a complete colonoscopy was not performed. In addition, our study population may not be representative for a screening population of patients at average risk of developing CRC. Although our cohorts were relatively small, the 3+3 study design is a commonly used method to acquire information on dosing or timing of a new compound, while limiting the number of exposed patients. (*20*) A future study will need to determine whether indeed EMI-137 can improve the current adenoma detection rate in a larger general screening population.

In conclusion, this study shows that FME using EMI-137 appears to be safe and feasible from a dose-to-imaging interval of one hour to at least three hours. Ultimately, a trade-off may be required between maintaining an adequate TBR for lesion detection and a clinically acceptable dose-to-imaging interval. Our data supports further research on the potential benefit of EMI-137 within this time-frame in phase II/III clinical trials, to investigate the potential improvement in polyp detection rates in a general screening population.

FUNDING

The study was funded by Edinburgh Molecular Imaging Ltd. (EMI), Edinburgh, United Kingdom. The funder of the study had no influence on data collection, analysis or interpretation, nor in writing of the manuscript. The corresponding author had full access to all data and had final responsibility for the decision to submit for publication.

DISCLOSURE

WBN received an unrestricted research grant from SurgVision B.V. (Groningen, the Netherlands). The other authors declare no potential conflicts of interest.

ACKNOWLEDGEMENTS

We would like to thank the patients that have participated in the clinical study and Gert Jan Meersma, senior lab analyst, for performing the *in vitro* experiments.

KEY POINTS

Question

What is the optimal dose-to-imaging interval for fluorescence molecular endoscopy (FME) using the c-Met targeted fluorescent peptide EMI-137 for colorectal polyp detection?

Pertinent findings

In this clinical trial, we show that FME using EMI-137 appears to be safe and feasible for the detection of colorectal adenomas within a one-to-three hour dose-to-imaging interval, based on *in vivo* visualization of fluorescence, *in vivo* quantification of fluorescence through correction for tissue optical properties and an extensive *ex vivo* validation.

Implications for patient care

Our findings expand the dose-to-imaging window for the clinical application of EMI-137 and supports further research on EMI-137 within this timeframe to improve the polyp detection rate in a general screening population.

ABBREVIATIONS

CRC	Colorectal cancer
eFTR	Endoscopic full-thickness resection
EMR	Endoscopic mucosal resection
ESD	Endoscopic submucosal dissection
FME	Fluorescence molecular endoscopy
HD-WL	High definition white-light
HGD	High-grade dysplasia
IQR	inter quartile range
i.v.	Intravenous
LGD	Low-grade dysplasia
MDSFR/SFF	Multidiameter single-fiber reflectance/single-fiber fluorescence
MFI	Mean fluorescence intensity
ROI	Region of interest
SVEE	SurgVision Explorer Endoscope
TBR	Target-to-background ratio

REFERENCES

1. Arnold M, Sierra MS, Laversanne M, Soerjomataram I, Jemal A, Bray F. Global patterns and trends in colorectal cancer incidence and mortality. *Gut*. 2017;66:683.

2. Leslie A, Carey F, Pratt N, Steele R. The colorectal adenoma–carcinoma sequence. *Brit J Surg*. 2002;89:845-860.

3. Segnan N, Senore C, Andreoni B, et al. Baseline Findings of the Italian multicenter randomized controlled trial of "once-only sigmoidoscopy" – SCORE. *J Natl Cancer Inst*. 2002;94:1763-1772.

4. Atkin W, Wooldrage K, Parkin MD, et al. Long term effects of once-only flexible sigmoidoscopy screening after 17 years of follow-up: the UK flexible sigmoidoscopy screening randomised controlled trial. *Lancet*. 2017;389:1299-1311.

5. Stoffel EM, Turgeon KD, Stockwell DH, et al. Missed adenomas during colonoscopic surveillance in individuals with Lynch syndrome (hereditary nonpolyposis colorectal cancer). *Cancer Prev Res*. 2008;1:470-475.

6. van Rijn JC, Reitsma JB, Stoker J, Bossuyt PM, van Deventer SJ, Dekker E. Polyp miss rate determined by tandem colonoscopy: a systematic review. *Am J Gastroenterol*. 2006;101:343-350.

7. Bressler B, Paszat LF, Vinden C, Li C, He J, Rabeneck L. Colonoscopic miss rates for right-sided colon cancer: A population-based analysis. *Gastroenterology*. 2004;127:452-456.

8. Burggraaf J, Kamerling IM, Gordon PB, et al. Detection of colorectal polyps in humans using an intravenously administered fluorescent peptide targeted against c-Met. *Nat Med*. 2015;21:955-961.

9. Joshi BP, Dai Z, Gao Z, et al. Detection of sessile serrated adenomas in the proximal colon using wide-field fluorescence endoscopy. *Gastroenterology*. 2017;152:1002-1013.

10. Hartmans E, Tjalma J, Linssen MD, et al. Potential Red-Flag Identification of colorectal adenomas with wide-field fluorescence molecular endoscopy. *Theranostics*. 2018;8:1458-1467.

11. Bradley CA, Dunne PD, Bingham V, et al. Transcriptional upregulation of c-MET is associated with invasion and tumor budding in colorectal cancer. *Oncotarget*. 2016;7:78932-78945.

12. Organ S, Tsao M-S. An overview of the c-MET signaling pathway. *Ther Adv Med Oncol*. 2011;3:S7-S19.

13. van Zaane LF, Gamm U, van Driel P, et al. In vivo quantification of the scattering properties of tissue using multi-diameter single fiber reflectance spectroscopy. *Biomed Opt Express*. 2013;4:696-708.

14. Hoy CL, Gamm UA, Sterenborg HJ, Robinson DJ, Amelink A. Method for rapid multidiameter single-fiber reflectance and fluorescence spectroscopy through a fiber bundle. *J Biomed Opt*. 2013;18:107005-107005.

15. Tjalma JJ, Koller M, Linssen MD, et al. Quantitative fluorescence endoscopy: an innovative endoscopy approach to evaluate neoadjuvant treatment response in locally advanced rectal cancer. *Gut*. 2020;69:406-410.

16. Nagengast WB, Hartmans E, Garcia-Allende PB, et al. Near-infrared fluorescence molecular endoscopy detects dysplastic oesophageal lesions using topical and systemic tracer of vascular endothelial growth factor A. *Gut*. 2019;68:7-10.

17. Esfahani SA, Heidari P, Kim SA, et al. Optical imaging of mesenchymal epithelial transition factor (MET) for enhanced detection and characterization of primary and metastatic hepatic tumors. Theranostics. 2016;6:2028–38.

18. Keller R, Winde G, Terpe H, Foerster E, Domschke W. Fluorescence dndoscopy using a fluorescein-labeled monoclonal antibody against carcinoembryonic antigen in patients with colorectal carcinoma and adenoma. *Endoscopy*. 2002;34:801-807.

19. Koch M, Symvoulidis P, Ntziachristos V. Tackling standardization in fluorescence molecular imaging. *Nat Photonics*. 2018;12:505-515.

20. Le Tourneau C, Lee JJ, Siu LL. Dose escalation methods in phase I cancer clinical trials. *J Natl Cancer Inst*. 2009;101:708-720.

FIGURES

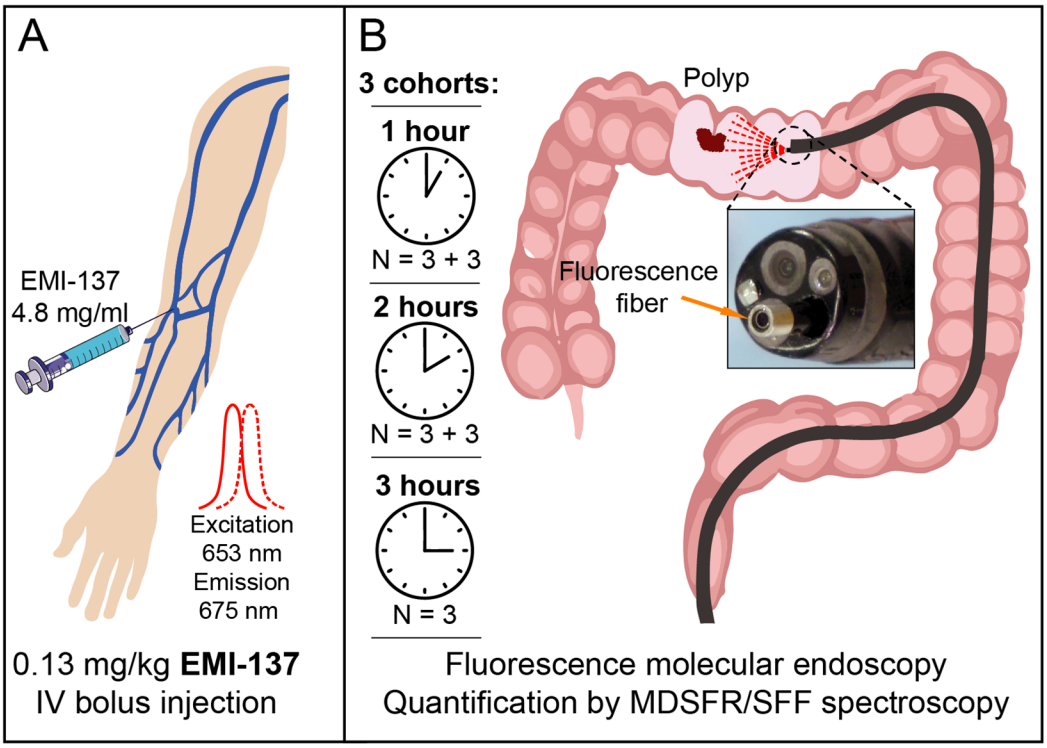

FIGURE 1. Study workflow. (A) EMI-137 was administered intravenously (0.13 mg/kg). (B) After one, two or three hours, real-time fluorescence molecular endoscopy (fiber-based fluorescence camera) and *in vivo* quantification of fluorescence (multi-diameter single-fiber reflectance, single-fiber fluorescence (MDSFR/SFF) spectroscopy) were performed. Per cohort, three patients were included, with expansion to six patients for the one and two hour cohort based on the interim analysis results.

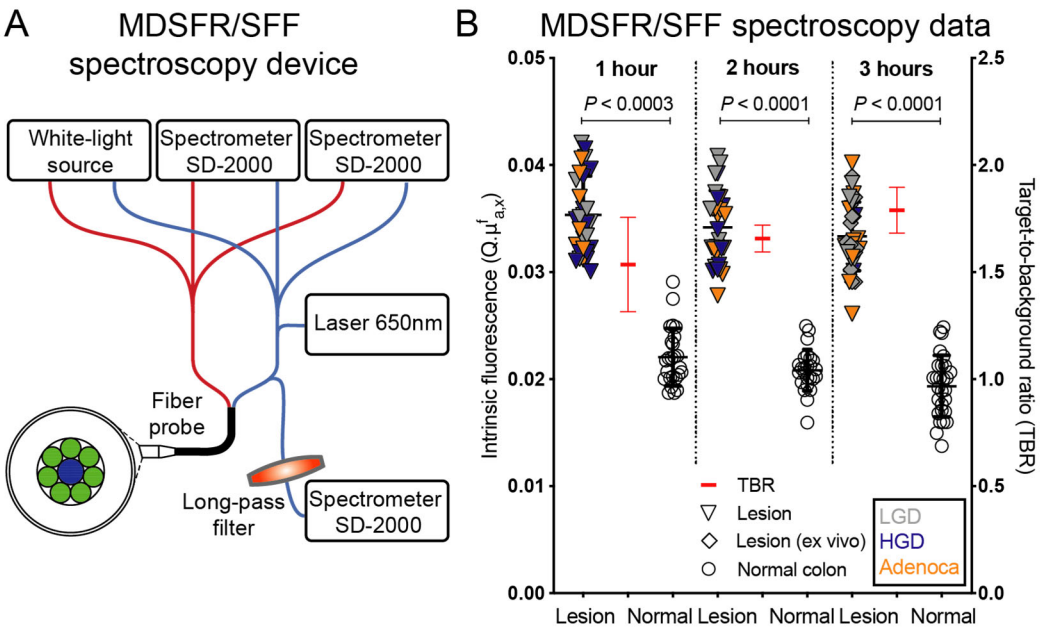

FIGURE 2. Multidiameter single-fiber reflectance, single-fiber fluorescence (MDSFR/SFF) spectroscopy. (A) Schematic overview of the device. (B) Individual intrinsic fluorescence values of the adenomas and surrounding normal tissue per time-cohort (left y-axis), with mean target-to-background (TBR) ratios (red; right y-axis). Histological grade of the adenoma: low-grade dysplasia (LGD; grey), high-grade dysplasia (HGD; blue) and adenocarcinoma (Adenoca; orange). Error bars: mean values ± standard deviation.

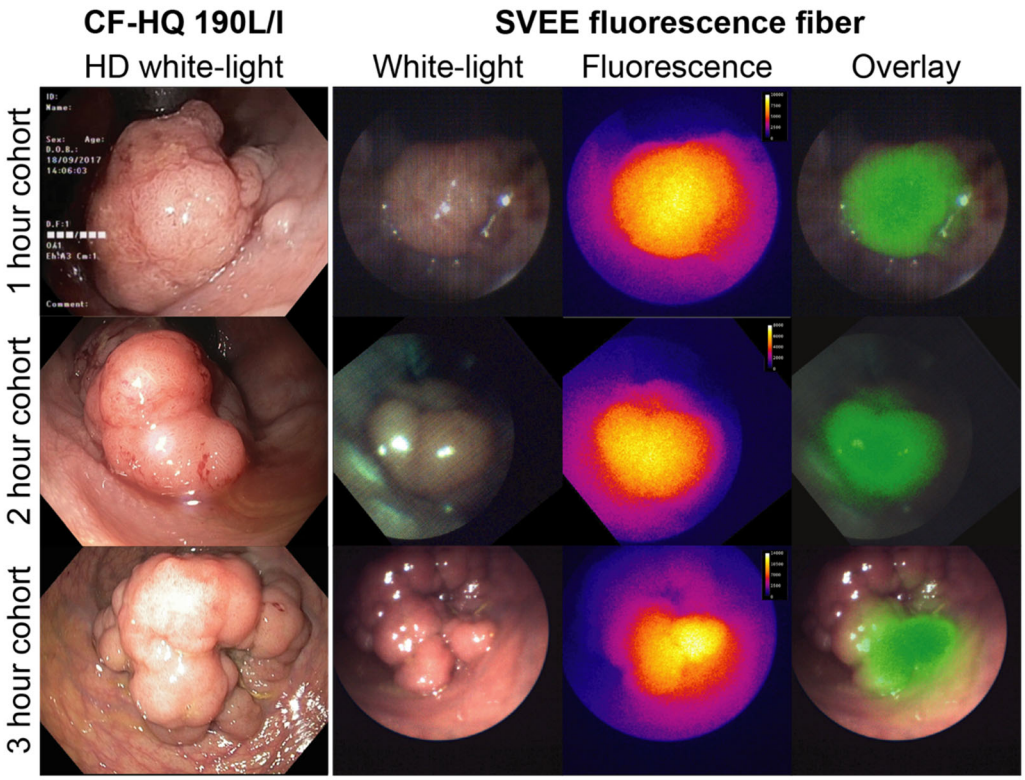

FIGURE 3. Fluorescence Molecular Endoscopy (FME). Representative FME images of a lesion with surrounding normal tissue for each cohort. Columns from left to right: high-definition (HD) white-light endoscopy image (Olympus CF-HQ 190L/I) and a white-light, fluorescence and overlay image (SurgVision Explorer Endoscope (SVEE)). Histology from top to bottom: adenocarcinoma, adenocarcinoma and low-grade dysplasia.

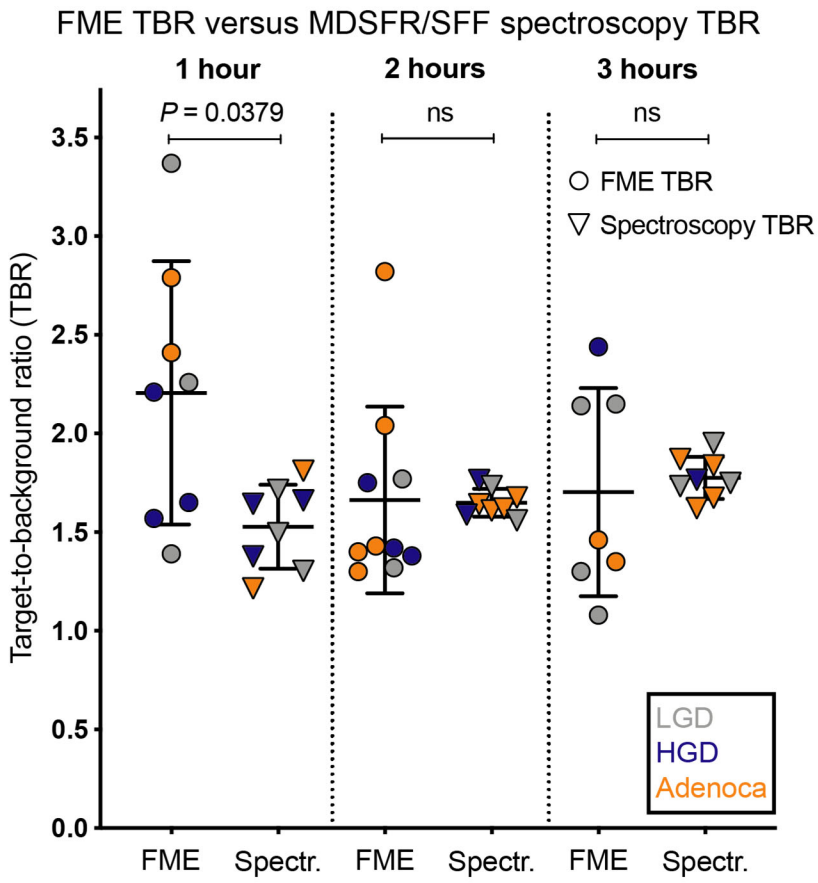

FIGURE 4. FME and MDSFR/SFF spectroscopy target-to-background ratios (TBR). Median TBRs of the fluorescence molecular endoscopy (FME) images and MDSFR/SFF spectroscopy data per time-cohort. Histological grade of the adenoma: low-grade dysplasia (LGD; grey), high-grade dysplasia (HGD; blue) and adenocarcinoma (Adenoca; orange). Error bars: median values ± IQR (FME TBRs) and mean ± standard deviation (MDSFR/SFF spectroscopy TBRs).

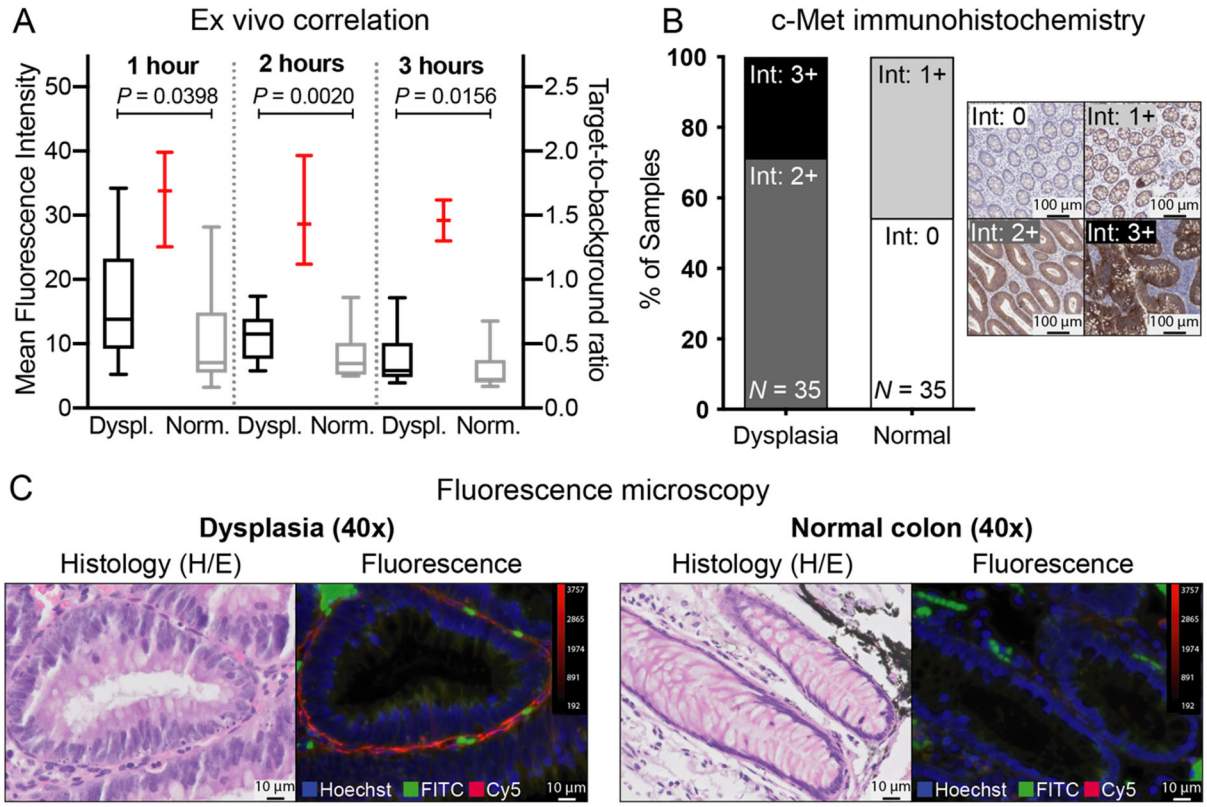

FIGURE 5. *Ex vivo* validation of EMI-137 fluorescence. (A) Correlation of mean fluorescence intensities of adenomatous (Dyspl). and surrounding normal tissue (Norm.) with histology on 4 µm tissue sections (*N* = 35), with median values ± IQR (left y-axis) and median target-to-background ratios (right y-axis; red). (B) c-Met membrane expression related to histology, with 0 = negative; 1+ = weak; 2+ = moderate and 3+ = strong membrane expression. (C) Fluorescence microscopy of dysplasia (left) and normal colorectal tissue (right). 40x magnification; DAPI/Hoechst nuclei staining (blue); FITC/autofluorescence (green) and Cy5/EMI-137 derived fluorescence (red).

TABLE

Patient characteristics	N=15 No.	%
Sex		
Male	10	66.7%
Female	5	33.3%
Age (years)		
Median (range)	62 (59-73)	
Body-Mass Index (kg/m^2)		
Median (range)	27.7 (21.6-42.7)	
Time cohort		
1 hour	6	40%
2 hours	6	40%
3 hours	3	20%
Endoscopy procedure		
Diagnostic	1	6.7%
Piecemeal polypectomy	3	20%
Endoscopic mucosal resection	4	26.6%
Endoscopic submucosal resection	6	40%
Endoscopic full-thickness resection	1	6.7%
Adenoma size (cm)		
Median (range)	3.0 (1.5-5.5)	
Histology (highest grade)		
Low-grade dysplasia	8	50%
High-grade dysplasia	5	31.2%
Adenocarcinoma	3	18.8%

TABLE 1. Demographics and clinical characteristics.

SUPPLEMENTARY MATERIAL

***Ex Vivo* Validation Side Study**

To confirm EMI-137 binding specificity, we performed in vitro experiments using two human colorectal cell lines: one with high c-Met overexpression (HT-29) and one with negative c-Met expression (SW-480) as a control. Cells were cultured in Gibco RPMI medium with 10% fetal calf serum (Bodinco BV, Alkmaar, The Netherlands). Cell lines were tested to be mycoplasma free by short tandem repeat profiling at Eurofins Genomics (Germany) and were kept in culture for a maximum of 50 passages. Briefly, c-Met membrane expression levels were analyzed in both cell lines by immunohistochemistry using a c-Met specific mouse-monoclonal antibody (sc-514148 clone D-4, Santa Cruz Biotechnology). Fluorescence microscopy was performed as a qualitative visual comparison and to demonstrate EMI-137 binding location at a microscopic level. Fluorescence-activated cell sorting (FACS) analysis was performed to confirm the specificity of the tracer and to measure its binding affinity to the c-Met receptor by a binding and blocking experiment.

C-Met membrane expression levels were analyzed in both cell lines by immunohistochemistry using a c-Met specific mouse-monoclonal antibody (sc-514148 clone D-4, Santa Cruz Biotechnology). For this purpose, cells were incubated in a 1:500 dilution for 1 hour at room temperature. Western blotting was performed to confirm the qualitative c-Met expression on a protein level, as reported previously. (*17*) The cells were incubated overnight at 4°C with the same antibody (sc-514148) in a 1:500 dilution and a mouse anti-actin monoclonal antibody (Clone: C4, MP biomedicals, Santa Ana, CA, USA) in a 1:10.000 dilution as a control. A secondary antibody was used to incubate the membrane (rabbit anti mouse-HRP, DAKO, Santa Clara, CA, USA) in a 1:1.500 dilution for 1 hour.

Subsequently, fluorescence microscopy was performed as a qualitative visual comparison and to demonstrate EMI-137 binding location at a microscopic level. After seven hours incubation in a serum-free phenol-red free RPMI medium at 37°C, cells were washed with 4°C PBS and

detached using a Gibco PBS-based enzyme-free cell dissociation buffer at room temperature. Cells were incubated with 10μg of EMI-137 or with medium alone as internal control at 37°C for five minutes. The cells were concentrated after washing steps using a cytospin and stained with 100μl of modified Kaisers glycerin in combination with a 0.5μg/ml Hoechst nuclei staining. Fluorescence microscopy was performed at a 63x magnification with fixed settings using a DM6000 fluorescence microscope coupled to a DFC360FX camera (Leica Microsystems, Wetzlat, Germany).

Fluorescence-activated cell sorting (FACS) analysis was performed to confirm the specificity of the tracer and to measure its binding affinity to the c-Met receptor. Both cell lines were prepared as described previously and subsequently incubated with four different concentrations of EMI-137 (0.5, 5, 50 and 500nM) in room temperature for 20 minutes. (*17*) In addition, blocking of the c-Met receptor was performed using the non-fluorescent unlabeled peptide (AH111972) in concentrations of 50nM, 500nM, 5μM and 50μM to demonstrate binding affinity. FACS-analyses were performed using the Accuri C6 flow cytometer (BD Biosciences, San Jose, CA, USA). Data analysis was performed using BD Accuri C6 software version 1.0.264.21. All of the above described experiments were repeated in triplicate for both cell lines.

SUPPLEMENTAL FIGURES

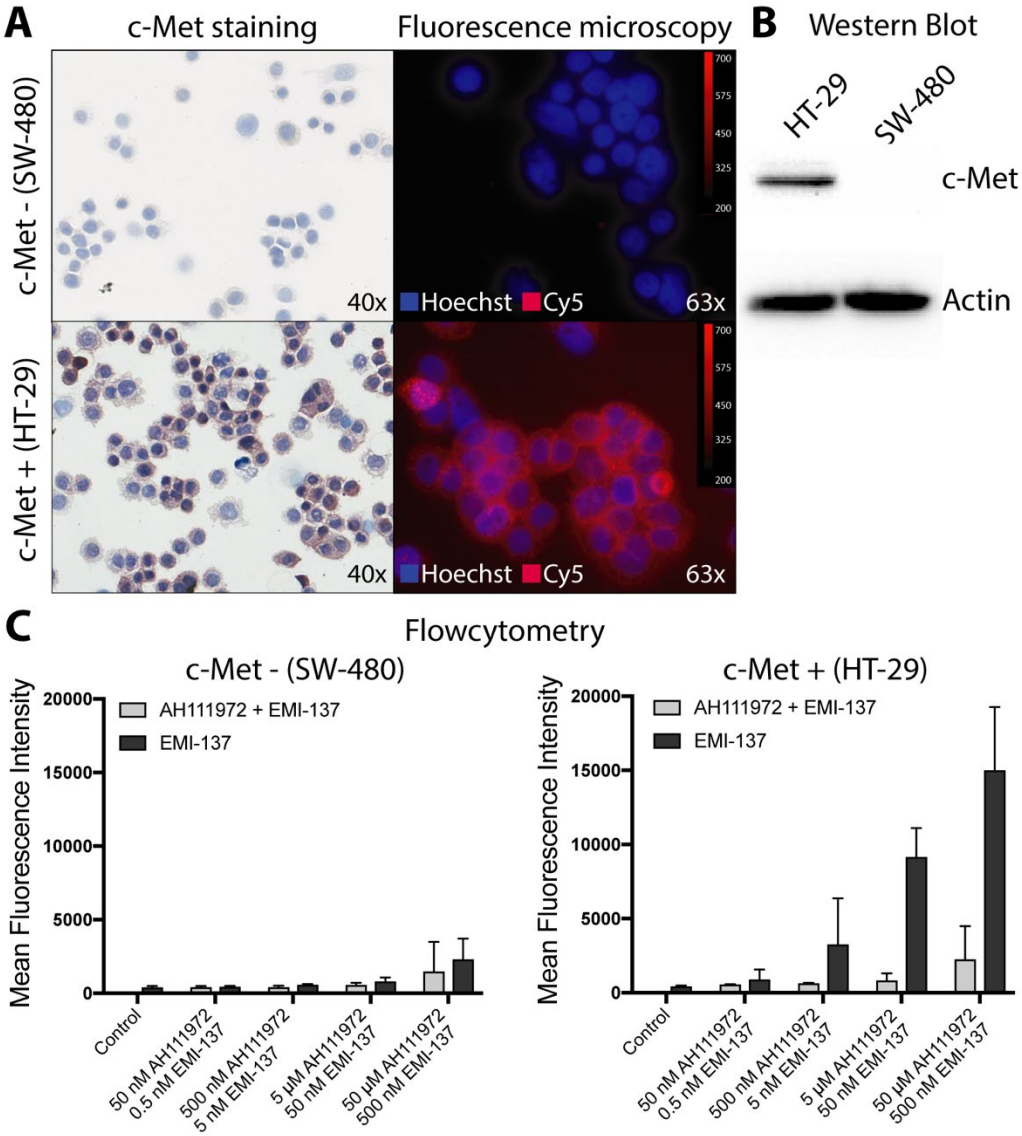

SUPPLEMENTARY FIGURE 1. *In vitro* experiments. (A) c-Met staining and fluorescence microscopy of the SW-480 (minimal c-Met expression) and HT-29 (high c-Met expression) colorectal cancer cell lines, showing clear c-Met overexpression and specific binding of EMI-137 in the HT-29 cell line. (B) Western Blot analysis confirming high c-Met expression in the HT-29 cell line and minimal-to-negative c-Met expression in the SW-480 cell line. (C) Flowcytometry of both cell lines using increasing concentrations of the unlabeled peptide (AH111972) and EMI-137, showing blocking of the c-Met receptor by the unlabeled peptide (AH111972 + EMI-137, light

grey), while EMI-137 only binds to the c-Met expressing HT-29 cell line (dark grey). Error bars represent median values with interquartile range. All experiments were performed in triplicate.